The geometry of the double-pulsar system J0737-3039 from systematic intensity variations.

Fredrick A. Jenet[1] & Scott M. Ransom[2,3]

[1] *California Institute of Technology, Jet Propulsion Laboratory, 4800 Oak Grove Drive, Pasadena, CA 91109; merlyn@alum.mit.edu*

[2] *McGill University Physics Dept., Montreal, QC H3A 2T8, Canada; ransom@physics.mcgill.ca*

[3] *Center for Space Research, Massachusetts Institute of Technology, Cambridge, MA 02139*

The recent discovery of J0737-3039A[1] & B[2]-two pulsars in a highly relativistic orbit around one another - offers an unprecedented opportunity to study the elusive physics of pulsar radio emission. The system contains a rapidly rotating pulsar with a spin period of 22.7 ms and a slow companion with a spin period of 2.77 s, hereafter referred to as 'A and 'B, respectively. A unique property of the system is that the pulsed radio flux from B increases systematically by almost two orders-of-magnitude during two short portions of each orbit[2]. Here, we describe a geometrical model of the system that simultaneously explains the intensity variations of B and makes definitive and testable predictions for the future evolution of the emission properties of both stars. Our model assumes that B's pulsed radio flux increases when illuminated by emission from A. This model provides constraints on the spin axis orientation and emission geometry of A and predicts that its pulse

profile will evolve considerably over the next several years due to geodetic precession until it disappears entirely in 15-20 years.

The double-pulsar system is extremely compact (orbital period, $P_{orb} \approx 2.45$h), mildly eccentric ($e \approx 0.088$), and highly inclined ($i > 87^o$). The orbital light curve shows two regions that last for about 12 min (30^o of orbital phase) and are separated by approximately 74^o where the pulsed radio flux of B increases dramatically[2]. The average pulse profile of A is composed of two peaks of width $20^o - 30^o$ separated by about 150^o in pulse phase[1].

We report on a model that explains the pulsed intensity variations seen in the orbital light curve of B using two simple assumptions. First, we assume that the emission geometry of A is given by the traditional hollow cone model of Lyne & Manchester[3] (see figure 1), and second, that B appears bright only when the emission beam of A illuminates it (i.e. when the cone of emission from A intersects B's position in the orbital plane). The key feature of the second assumption, which we call the "stimulated emission hypothesis", is that the particles and/or electromagnetic radiation from A which stimulate the radio emission from B are directed along the same emission cone as A's observed radio radiation. These two assumptions enable one to derive a set of non-linear equations (see the caption to figure 1) that determines how the conal emission from A intersects with our line-of-sight, how it projects onto the orbital plane, and when it illuminates B. These five equations contain a total of 11 variables, six of which are obtained from observations, and which therefore allow us to solve for the five unknowns. The six measured parameters are the orbital inclination angle, i, the angle

between the outer edges of the double peaked pulse profile, P_o, the angle between the inner edges of the peaks in the pulse profile, P_i, the angle between the outer edges of the double peaked orbital light curve, O_o, the angle between the inner edges of the orbital light curve, Oi, and the midpoint of the orbital light curve, O_m. The angles obtained by solving the five constraint equations are λ and ϕ which are the polar angles that determine the orientation of the spin axis with respect to the orbital angular momentum (see figure 1), and ρ, α, and δ, which determine the emission geometry (see figure 2).

Table 1 lists the adopted values of the measured parameters i, P_i, P_o, O_i, O_o, and O_m. These values were obtained from 427, 820, 1400, and 2200 MHz data taken with the Green Bank Telescope[4]. These observations, which cover a factor of 5 in radio frequency, indicate that the pulse profile of A and the orbital light curve of B are both effectively independent of observing frequency for our purposes. Given the measured parameters, we solved the constraint equations and found two solution sets for the five unknown angles, which are also listed in Table 1. These two solutions exist due to the uncertainties in the measured parameters. A video showing the relative motions of the pulsars, the intersection of A's conal emission with the orbital plane for solution 1, and the regions of enhanced emission from B is available on-line[5].

In our model, the orientation of A's spin axis plays a major role in determining the shape of both the pulse profile of A and the orbital light curve of B. Geodetic precession[6,7], caused by the curvature of space-time around the pulsars, will cause the spin axis to precess about the orbital angular momentum vector, $\mathbf{J}$, at a rate of 4.77^o per year. Hence, the angle ϕ will increase at this rate while the four other inferred angles

will remain constant. Consequently, we can predict the future evolution of both the orbital light curve and the pulse profile of A. Given the inferred values of λ, ϕ, ρ, α and δ together with a value of ϕ at a specified time, the five constraint equations determine the pulse profile parameters, P_i, and P_o, and the orbital light curve parameters O_o, O_i, O_m. Both O_i and O_o will remain constant while O_m, which is equal to ϕ, will increase at a rate of 4.77^o per year. This effect will be easily measurable over the next 1-2 years. The geodetic precession will also cause highly significant pulse profile changes over timescales of a few years (see figure 3). Note that similar, although smaller amplitude, precession-induced profile changes have already been observed in the binary system PSR B1913+16[8,9]. For solution 1, P_o and P_i will increase by $42^o \pm 16^o$ and $31^o \pm 8^o$ in 1 year , respectively. For solution 2, P_o and P_i will increase by $96^o \pm 13^o$ and $34^o \pm 6^o$ in one year, respectively. For both solutions, P_o, will approach its maximum extent, 3600, in less than 2 years. Pulsar A is expected to disappear in about 14 years according to solution 1. For solution 2, the pulsar will disappear in approximately 4.5 years and then reappear in 10 years as a single-peaked pulsar (temporarily) where it will remain "on" for 6-7 years. For both solutions, we estimate that the pulsar came into view approximately 4-5 years in the past. This can explain why the Parkes 70-cm survey for pulsars, completed in 1997, did not detect this system in spite of sufficient sensitivity and appropriate sky coverage[10].

Recently, Demorest et al.[11] used the polarization properties of A together with the standard rotating vector model of Radhakrishnan & Cooke[12] in an attempt to measure its emission geometry. Due to limitations in both the model and the data, they were

only able to measure the angle α which they found to be $4^o \pm 3^o$. This result is consistent with our solution 1. Since they only measured one of the five angles needed to completely specify the geometry, they were unable to predict the future evolution of the emission properties of this system.

We note that the current form of the model does not consider the precession of B. However, it is likely that wind-torques from A, which dominates the system energetically, have caused the spin axis of B to align with the direction of the orbital angular momentum[13,14]. In this case, geodetic precession will have no effect on the emission from B. It is also possible that the direction of B's emission beam may lie in the orbital plane as a result of the stimulated emission process regardless of the magnetic field alignment. In this scenario, geodetic precession would also have little effect on the direction of B's emission.

Given that the model presented here accurately describes the current data, it becomes important to understand the physics behind the stimulation process. Future work will explore various possible mechanisms. One idea involves "jump-starting" the pulsar emission processes in B by initiating electron-positron pair cascades in its magnetosphere that emit coherent radio emission. The initiating particles could be the positrons and electrons emitted in the wind of A, or, more likely, gamma rays that are expected to be travelling in nearly the same direction as the radio photons. Alternatively, pressure from a conal A-wind could distort B's magnetosphere[14] and push its beam more directly into our line of sight.

1. Burgay, M., D'Amico, N., Possenti, A., Manchester, R. N., Lyne, A. G., Joshi, B. C., McLaughlin, M. A., Kramer, M., Sarkissian, J. M., Camilo, F., Kalogera, V., Kim, C., & Lorimer, D. R. An increased estimate of the merger rate of double neutron stars from observations of a highly relativistic system. Nature, **426**, 521-533 (2004)

2. Lyne, A. G., Burgay, M., Kramer, M., Possenti, A., Manchester, R. N., Camilo, F., McLaughlin, M. A., Lorimer, D. R., D'Amico, N., Joshi, B. C., Reynolds, J., Freire, P. C. C., A Double-Pulsar System - A Rare Laboratory for Relativistic Gravity and Plasma Physics. Science, **303**, 1153-1157 (2004)

3. Lyne, A. G., Manchester, R. N., The shape of pulsar radio beams. Mon. Not. R. Astron. Soc., **234**, 477-508 (1988)

4. Ransom, S., Kaspi, V., Demorest, P., Ramachandran, R., Backer, D., Pfahl, E., Ghigo, F., Arons, J., Kaplan, D. Green Bank Telescope Measurement of the Systemic Velocity of the Double Pulsar Binary J0737-3039 and Implications for its Formation, Astrophys. J., submitted (2004)

5. http://www.physics.mcgill.ca∼ransom/0737_Bflux_model.mpg

6. Barker, B. M. & O'Connell, R. F., Gravitational two-body problem with arbitrary masses, spins, and quadrupole moments, Phys. Rev. D., **12**, 329-335 (1975)

7. Barker, B. M. & O'Connell, R. F., Relativistic effects in the binary pulsar PSR 1913+16, Astrophys. J., **199**, L25-L26 (1975)

8. Kramer, M., Determination of the Geometry of the PSR B1913+16 System by Geodetic Precession, Astrophys. J., **509**, 856-860 (1998)

9. Weisberg, J. M. & Taylor, J. H., General Relativistic Geodetic Spin Precession in Binary Pulsar B1913+16: Mapping the Emission Beam in Two Dimensions, Astrophys. J., **576**, 942-949 (2002)

10. Lyne, A. G., Manchester, R. N., Lorimer, D. R., Bailes, M., D'Amico, N., Tauris, T. M., Johnston, S., Bell, J. F., Nicastro, L., The Parkes Southern Pulsar Survey - II. Final results and population analysis., Mon. Not. R. Astron. Soc., **295**, 743-755 (1998)

11. Demorest, P., Ramachandran, R., Backer, D. C., Ransom, S. M., Kaspi, V., Arons, J., Spitkovsky, A., Orientations of Spin and Magnetic Dipole Axes of Pulsars in the J0737-3039 Binary Based on Polarimetry Observations at the Green Bank Telescope. Astrophysics J., submitted, astro-ph/0402025 (2004)

12. Radhakrishnan, V., Cooke, D. J., Magnetic Poles and the Polarization Structure of Pulsar Radiation. Astrophys. J., **3**, L225-L228 (1969)

13. Kaspi, V. M., Ransom, S. M., Backer, D. C., Ramachandran, R., Demorest, P., Arons, J., Spitkovskty, A., Green Bank Telescope Observations of the Eclipse of Pulsar B in the Double Pulsar Binary PSR J0737-3039. Astrophys. J., submitted, astro-ph/0401614 (2004)

14. Arons, J., Spitkovskty, A., Backer, D., Kaspi, V. Probing Relativistic Winds and

Magnetospheres: Torques and Eclipses of PSR J0737-3039 A & B. Astrophys. J., submitted (2004)

15. Press, W. H., Flannery, B. P., Teukolsky, S. A. & Vetterling, W. T. *Numerical Recipes in C. The Art of Scientific Computing* (Cambridge Univ. Press, 1988).

Correspondence and requests for materials should be addressed to F. J. (merlyn@alum.mit.edu)

Competing interests statement The authors declare that they have no competing financial interests.

Acknowledgements Part of this research was performed at the California Institute of Technology's Jet Propulsion Laboratory, under contract with NASA and funded through the internal Research and Technology Development Program. The authors wish to thank Vicky Kaspi, John Armstrong, Jonathan Arons, Donald Backer, Paulo Freire, and Dick Manchester for useful discussions and comments. F. J. extends special thanks to Thomas A. Prince and E. B. Dussan V.

Table 1: Measured and Inferred Properties of J0737-3039

Measured Parameters			
Orbital Inclination	i	$88.5^o \pm 1.5^o$ or $91.5^o \pm 1.5^o$	
Profile outer width	P_o	$251^o \pm 10^o$	
Profile inner width	P_i	$109^o \pm 10^o$	
Orbital outer width	O_o	$110^o \pm 10^o$	
Orbital inner width	O_i	$22^o \pm 10^o$	
Orbital Midpoint	O_m	$246^o \pm 10^o$	
Inferred Parameters for $i = 88.5 \pm 1.5$		Solution 1	Solution 2
Spin Axis	λ	$167^o \pm 10^o$	$90^o \pm 10^o$
	ϕ	$246^o \pm 5^o$	$239^o \pm 2^o$
Magnetic field angle	α	$1.6^o \pm 1.3^o$	$14^o \pm 2^o$
Emission ring opening angle	ρ	$78^o \pm 8^o$	$42^o \pm 4^o$
Emission ring width	2δ	$1.9^o \pm 1.4^o$	$15^o \pm 2^o$
Total visible time		19 ± 2 yrs	19 ± 2 yrs
Time remaining		14 ± 2 yrs	4.5 ± 0.1 yrs
Predicted changes in 1 year		Solution 1	Solution 2
Change in P_o		$42^o \pm 16^o$	$96^o \pm 13^o$
Change in P_i		$31^o \pm 8^o$	$34^o \pm 6^o$
Change in O_o		0^o	0^o
Change in O_i		0^o	0^o
Change in O_m		$4.77^o \pm .01^o$	$4.77^o \pm .01^o$

Note - The measured and inferred geometric parameters for PSR J0737-3039. Timing[2] and scintillation[4] observations have determined i to be either $88.5^o \pm 1.5^o$ or $91.5^o \pm 1.5^o$. Two values are allowed since current data are unable to distinguish between i and $180^o - i$, although future timing observations should resolve this degeneracy. If a solution to the constraint equations exists for a given inclination, i, then a solution will also exist for an inclination of $180^o - i$. The only difference between the two solutions will be that λ will become $180^o - \lambda$. In the text, the results are presented only for the case $i < 90^o$ with the understanding that corresponding solutions also exist if $i > 90^o$. Note that the evolution of a given solution does not change when λ goes to $180^o - \lambda$. We estimated the errors in the inferred parameters by allowing the measured parameters (i, P_o, P_i, O_o, O_i, O_m) to vary by the given uncertainties and then calculating the variations in the resulting solutions. The solutions were found by solving the five non-linear constraint equations using Broyden's method[15]. An initial guess for each of the five angles was chosen at random and then refined using this algorithm. This was performed 10000 times in order to determine all possible solutions.

Figure 1 - The hollow cone model of radio pulsar emission. Ω is the spin axis of the pulsar, which is separated by the magnetic dipole axis μ by the angle α. The conal emission centered on μ has an opening half-angle ρ and is of angular thickness 2δ. The cut of an observer's line-of-sight through the cone as it rotates can produce either a single or double-peaked pulse profile. This emission geometry together with the stimulated emission hypothesis yield the following five constraint equations:

$$\sin(\lambda)\cos\left(\frac{O_i}{2}\right) = \begin{cases} \cos(\rho+\delta-\alpha) & ;\alpha \geq \rho+\delta \\ \sin(\lambda) & ;\rho-\delta < \alpha < \rho+\delta \\ \cos(\rho-\delta-\alpha) & ;\alpha \leq \rho-\delta \end{cases} \quad (1)$$

$$\sin(\lambda)\cos\left(\frac{O_o}{2}\right) = \cos(\rho+\delta+\alpha) \quad (2)$$

$$\phi = O_m \quad (3)$$

$$\cos(\rho-\delta) = A\cos(\alpha) + \sqrt{1-A^2}\sin(\alpha)\cos(P_i/2) \quad (4)$$

$$\cos(\rho+\delta) = A\cos(\alpha) + \sqrt{1-A^2}\sin(\alpha)\cos(P_o/2) \quad (5)$$

Here, $A = \cos(\lambda)\cos(i) - \sin(i)\sin(\lambda)\sin(\phi)$. P_i, P_o, O_i, O_o, O_m, and i are measured parameters defined in the text. λ and ϕ are defined in figure 2.

Figure 2 - The geometry of key orbital- and spin-related angles in the J0737-3039 system. Orthogonal axes representing the three spatial dimensions are denoted by **x** (the direction of the Line of Nodes in the orbital plane), **y** (the projected direction of the Line of Sight of an Earth-bound observer onto the orbital plane), and **z** (the direction anti-aligned with the angular momentum vector of the orbit, **J**). The pulsars orbit in the **x-y** plane in a clockwise direction. The orientation of the spin axis of J0373-3039A is Ω, which is separated by the

orbital angular momentum, **J**, by the angle λ, and the magnetic dipole axis, μ, by the angle α. The projection of Ω onto the orbital plane defines the angle ϕ. The line-of-sight of the observer is inclined by the inclination angle i from **J** in the **y-z** plane.

Figure 3 - A greyscale plot of the A pulsar pulse profile evolution as a function of time for both sets of solutions. The profile is given by a constant time slice. T=0 refers to January 1, 2004 (MJD= 53005.0). Since this model only determines the locations of the emission regions as opposed to the exact shape of the profile, the simulated pulse profiles are represented as square waves. We predict that the 'A' pulsar will disappear from view in about 14 years for solution 1 or about 4.5 years for solution 2. The lack of pulsed emission from either solution can explain the lack of detection of the pulsars during the Parkes 70-cm pulsar survey in the mid-1990s[6]. Note that we have only considered one emission cone emanating from one side of the A pulsar. Given the symmetries of a dipole magnetic field, it is possible that another emission cone, the "auxiliary cone", is emanating from the other magnetic pole. If it exists, this auxiliary cone may eventually appear as a new component in the pulsar profile of A due to geodetic precession. Its appearance, though, should not affect our predictions for the positioning of the components of the currently observed cone. In the framework of the stimulated emission hypothesis, the auxiliary cone will also induce emission from B. This "secondary" emission should appear at orbital phases approximately 180^o away from those at which enhanced emission is currently seen. Intriguingly, secondary emission from B has been reported from these orbital phases[11], but the enhancement factor is much smaller than that in the two bright regions. Absorption or scattering of the radio emission at the shock generated near B by the interaction between the plasma winds from stars could explain this effect. A similar shock is believed to cause the eclipses seen in A[13].

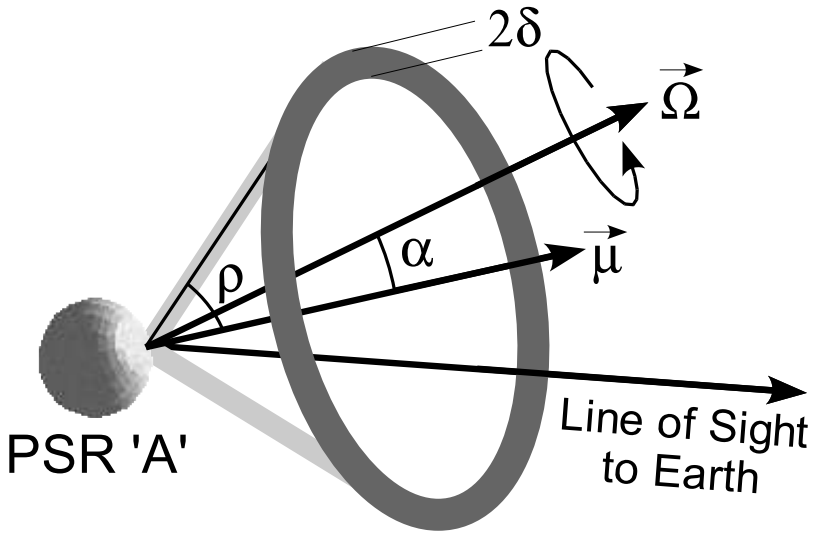

Figure 1

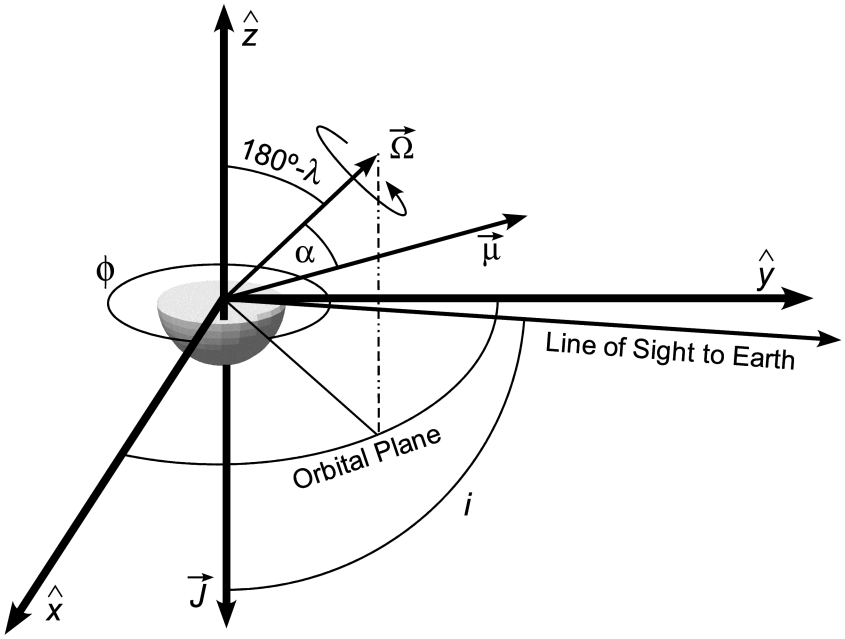
$\hat{z}$
180°-λ
$\vec{\Omega}$
α
$\vec{\mu}$
ϕ
$\hat{y}$
Line of Sight to Earth
Orbital Plane
i
$\vec{J}$
$\hat{x}$

Figure 2

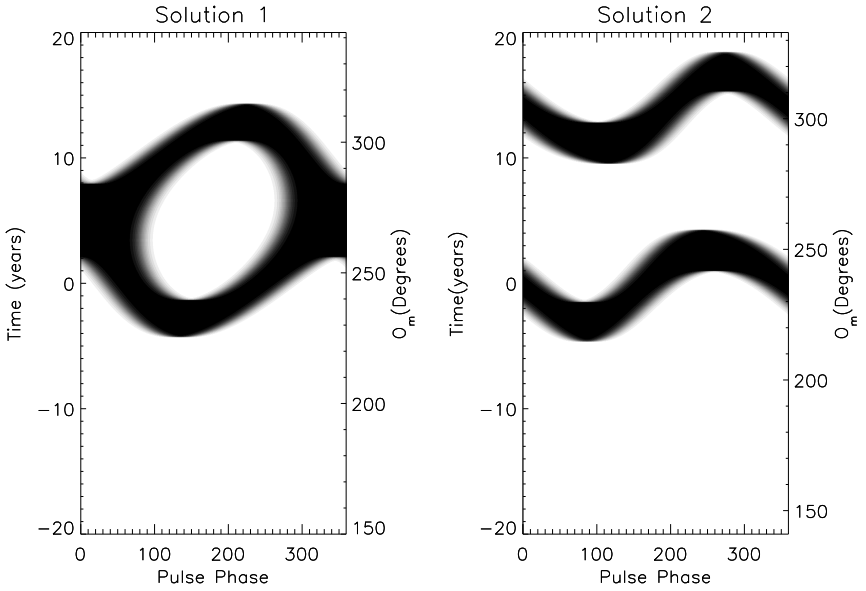
Solution 1
Solution 2
Time (years)
Time(years)
Pulse Phase
Pulse Phase
Ω_m(Degrees)
Ω_m(Degrees)
20
10
0
−10
−20
0
100
200
300
150
200
250
300

Figure 3